Applied Surface Science 616 (2023) 156438

Contents lists available at ScienceDirect

Applied Surface Science

journal homepage: www.elsevier.com/locate/apsusc

Full Length Article

Adsorption of water and organic solvents on the calcite [10$\bar{1}$4] surface: Implications for marble conservation treatments

Antonia E. Papasergio [a], Greta Ugolotti [b], Enrico Sassoni [b,*], Martina Lessio [a,*]

[a] School of Chemistry, University of New South Wales, Kensington, 2052 New South Wales, Australia
[b] Department of Civil, Chemical, Environmental and Materials Engineering (DICAM), University of Bologna, Via Terracini, 28, 40131 Bologna, Italy

ARTICLE INFO

Keywords:
Marble conservation
Hydroxyapatite
Interface
Calcite
Water
Organic solvents
Density functional theory
Molecular dynamics

ABSTRACT

When exposed outdoors, marble artefacts are subject to degradation caused by dissolution in rain. To improve acid-resistance of marble, surface treatments involving the *in situ* formation of a passivating calcium phosphate (CaP) layer have been developed. Adding alcohol to the treatment improves CaP coverage but the reason is still unclear. Here, we use computational and experimental studies to ascertain whether the interaction of the organic additives with the marble surface plays a role in determining the treatment outcome. Density functional theory calculations are employed to determine the binding energy of additives on the calcite [10$\bar{1}$4] surface and identify acetone as a promising new additive due to its weak adsorption. Molecular dynamics calculations show that ethanol and isopropanol displace water from the calcite [10$\bar{1}$4] surface forming an immobile, ordered, and hydrophobic layer, while acetone and water form a mixed, dynamic environment. In experimental trials, a continuous (yet cracked) layer of carbonate hydroxyapatite is formed after 24 h, with all organic additives improving the final coating. This result suggests that the interaction of the additive with the marble surface does not play a major role in determining treatment outcomes and other factors should be investigated for the design of improved treatments.

1. Introduction

Calcium carbonate ($CaCO_3$), especially in the form of calcite (the most stable polymorph of calcium carbonate), plays a fundamental role in many fields. In particular, calcite/liquid interfaces govern processes occurring in natural sciences (*e.g.*, geochemistry, ocean chemistry, biomineralization by marine organisms) and technology (*e.g.*, CO_2 storage, energy, medicine, catalysis) [1–3]. Aside from these fields, calcite/liquid interfaces are also important to cultural heritage conservation, as calcite is the principal component of many historical materials used in sculpture and architecture which are exposed to the outdoor environment [4].

Among calcite-based materials, marble is highly prized for its aesthetic qualities and, as such, has been used in many artefacts of cultural significance around the world. When situated outdoors, marble artefacts are prone to deterioration due to dissolution in rain, a consequence of the aqueous solubility of calcite (the solubility product at 25 °C being $K_{sp} = 5{\cdot}10^{-9}$ and the dissolution rate being $\sim 10^{-10}$ mol/(cm^2·s) at pH 5.6 [4,5]). Rainwater is naturally acidic, further increasing calcite's dissolution rate [4]. Damage to marble artefacts caused by dissolution ranges from microscopic surface corrosion to a loss of mechanical integrity and noticeable aesthetic changes. To improve acid-resistance of marble, numerous organic or inorganic surface coatings have been tested through the years [6]. However, most have proved dissatisfactory due to substrate incompatibility, poor durability or visible aesthetic change [7].

In recent years, a promising new treatment involving the *in situ* formation of a new mineral layer composed of calcium phosphate (CaP) (ideally hydroxyapatite, HAP, $Ca_{10}(PO_4)_6(OH)_2$) has been developed. The new CaP surface layer is formed by reaction of marble with an aqueous solution of diammonium hydrogen phosphate (DAP) and an additional calcium source ($CaCl_2$), ideally forming a coherent and durable layer improving acid-resistance of the substrate [8]. HAP is the preferred CaP for protection and consolidation of calcite grains; it has a good crystal lattice match, similar crystal structure, reduced solubility and slower dissolution rate, is the most stable CaP at pH > 4, and causes no observable aesthetic change to the treated substrate [7].

Recently, it was found that the addition of alcohol (ethanol or isopropanol) to the reaction mixture improves CaP coverage [9–10], yet the

* Corresponding authors.
E-mail addresses: enrico.sassoni2@unibo.it (E. Sassoni), martina.lessio@unsw.edu.au (M. Lessio).

https://doi.org/10.1016/j.apsusc.2023.156438
Received 5 December 2022; Received in revised form 4 January 2023; Accepted 13 January 2023
Available online 18 January 2023

reason for this improvement is unclear. The addition of the alcohols is thought to have two competing effects: a beneficial one in solution and a negative one at the surface. In solution, alcohols are thought to weaken the hydration sphere of phosphate ions thereby reducing the energy needed for dehydration, [11] as well as increasing the supersaturation of the solution, aiding the precipitation of CaP [12] which may be productive to the *in situ* growth of CaP. At the surface of calcite, ethanol and isopropanol are known to displace adsorbed water, [13–16] thereby reducing the wettability of calcite which may be counterproductive for the nucleation of CaP.

The general aim of this paper is to elucidate the effect that organic additives have at the calcite surface and shed light on which of the two competing effects discussed above is predominant, thus aiding the improvement of the conservation treatment. Density functional theory (DFT) calculations are employed to determine the adsorption geometry and relative binding strength on the calcite surface of single molecules important to the protective treatment. The results of these simulations allow us to identify acetone as a new promising organic additive. Subsequently, we use classical molecular dynamics (MD) calculations to model the interaction between solvent solutions and the calcite surface. These calculations better reflect experimental conditions and the competitive adsorption environment, thus providing insights on the wettability of the calcite surface, which is critical for the nucleation of CaP. Based on the results of the computational studies, we perform experiments to compare the performance of the acetone, the newly proposed additive, to ethanol, isopropanol, and water (as a reference). The outcome of these experiments allows us to ascertain whether the adsorption of the additive on the calcite surface has a major impact on the treatment outcome and should thus be considered as a critical factor when choosing an additive for conservation treatments of marble. Furthermore, alongside the specific field of cultural heritage, the findings of the present study can provide useful insights to the many fields where calcite/liquid interfaces are of interest, such as geoscience, biomineralization, and medicine, especially when organic additives are involved.

2. Materials and methods

2.1. Computational methods

2.1.1. Density functional theory

All calculations were performed with periodic boundary conditions (PBC) using the VASP code [17–19], and DFT [20–21] using the PBE exchange-correlation functional [22]. Nuclei (Ca, O, C and H) and frozen core electrons (1s2s2p3s for Ca, 1s for O and 1s for C) were modelled using default projector augmented wave (PAW) potentials [23]. The remaining electrons were modelled using a plane wave basis set with a kinetic energy cut-off of 800 eV. All calculations were performed spin-polarised. We used DFT-D3(BJ) dispersion corrections [24] to improve the description of adsorbate-surface interactions. To sample the Brillouin zone, we used the Monkhorst-Pack scheme [25] with a k-point sampling mesh of $6 \times 6 \times 2$ for the bulk crystal, $2 \times 2 \times 1$ for the surface supercell, and $1 \times 1 \times 1$ for the isolated molecules. Integration of the Brillouin zone was performed using the Gaussian smearing method with a smearing width of 0.05 eV for the slab and 0.001 eV for isolated molecules. Structural optimisations were considered converged when the forces acting on each atom were smaller than 0.03 eV/Å.

The initial guesses for adsorption geometries were based on optimised geometries suggested by a previous study [14], however for each adsorbate, multiple initial geometries were sampled using the most stable configuration of the hydroxyl group of ethanol as a building-block. The surface coverage of each adsorbate was fixed at 0.25 monolayers (ML), *i.e.*, each unit cell had 4 Ca adsorption sites and 1 adsorbate was placed in each unit cell. Dipole corrections were implemented to prevent the event of spurious dipole formation in our asymmetric slab model.

The adsorption energy (E_{ads}) to the calcite surface was calculated as.

$$E_{ads} = E_{(adsorbate+slab)} - E_{adsorbate} - E_{slab}$$

where E_{slab}, $E_{adsorbate}$ and $E_{(adsorbate+slab)}$ are the energies of the isolated calcite slab, an isolated adsorbate molecule, and the complex formed by the molecule adsorbed onto the calcite surface, respectively. With this sign convention, a negative E_{ads} corresponds to favourable adsorption.

2.1.2. Molecular dynamics

The force field used in this study is a hybrid of Pavese, Amber, and TIP3P potentials, similar to that used by Cooke et al. and reported in Table S1-4 [26]. To model calcite, we implemented the Pavese et al. potential [27–28], which is dominated by non-bonding Coulombic and Buckingham potentials, with bond, angle, and improper terms to describe the carbonate groups. Organic solvents (ethanol, isopropanol, and acetone) were described using the GAFF force field [29]. Point charges were calculated using DFT within the Orca software package [30–31] with the CHELPG charge scheme. To model water, we used the TIP3P forcefield [32] parametrised for use with Ewald summation [33]. The non-bonded potentials between water/organic solvents were generated by applying standard Lorentz-Berthelot mixing rules. To validate the combination of GAFF and TIP3P force fields for modelling pure solvents and solvent mixtures, we benchmarked their computed density with experimental density measurements found in literature (see Table S7 in the Supporting Material). To improve the match to experimental data, we decreased acetone's point charges of oxygen (δ-) and hydrogen (δ+) by 20 %, and reduced σ of $O_{acetone}$-O_{water} by 20 %. The Buckingham potentials for $Ca_{calcite}$-$O_{organic/water}$ interactions were derived according to the methodology developed by Freeman et al. for describing non-bonded interactions between calcite and solvents [34]. This process has been used in similar studies of adsorption on the calcite surface [26,35]. The $O_{calcite}$-O_{water} interaction was described with a 9–6 Lennard-Jones potential based on the known structure of ikaite ($CaCO_3 \cdot 6H_2O$) as fit by Freeman and coworkers [34]. The $O_{calcite}$-$O_{calcite}$ 12–6 Lennard-Jones potential (derived by Freeman et al. from the Pavese $O_{calcite}$-$O_{calcite}$ Buckingham potential) was used in order to be able to derive all $O_{calcite}$-organic 12–6 Lennard-Jones interactions using the standard Lorentz-Berthold mixing rules. Similarly, the $C_{calcite}$-organic interactions were generated using the standard Lorentz-Berthold mixing rules with the same method as Freeman [34]. Due to the lack of a non-bonding repulsive term for $Ca_{calcite}$-$C_{organic}$, we encountered unphysical attractions between negatively charged aliphatic carbon sp^3 atoms and positively charged calcium ions (Ca^{2+}). To address this issue, we implemented a Buckingham repulsion term for Ca-C(H_3) as parametrised by Kim and coworkers in their study of decane adsorption on the calcite [$10\bar{1}4$] surface [35].

The Packmol code [36–37] was used to generate initial configurations by filling the vacant space between calcite slabs with the required number of solvent molecules (water, ethanol, isopropanol and acetone) corresponding to their calculated equilibrium density at 300 K for both pure solvents and solvent mixtures. To better understand competitive adsorption behaviour, three initial configurations of water/organic solvent mixtures at a constant concentration of 1:1 by number of molecules were used when filling the vacant space between the calcite layers; the first and second were three alternating controlled solvent layers with the layers adjacent to calcite comprised of either water or organic solvent, the third was mixed with a random spatial arrangement. We used the LAMMPS code [38] to perform the simulations and VMD [39] for analysis and visualisation. All calculations were run at 300 K and 1 bar with the Nosé-Hoover thermostat and a timestep of 0.5 fs. Long range coulombic interactions were calculated with Ewald summation [33]. The systems underwent an initial relaxation with an NVT ensemble for 0.05 ns, followed by an NPT ensemble with constrained calcite dimensions (*i.e.*, the cell was allowed to relax only in the z

direction) for 0.05 ns. After this brief initial relaxation period, we used an NPT ensemble to allow all atoms and cell dimensions to relax and ran an equilibration period of 2 ns, followed by a production run of 10 ns for the pure solvents and 20 ns for the 1:1 solvent mixtures. The brief initial constrained relaxation ensured that the solvents reached the correct density while avoiding distortion of the calcite cell parameters during the following equilibration and production runs. Molecular trajectories were sampled every 1 ps throughout the production run to monitor changes of properties over time and ensure convergence. Reported properties were calculated by averaging values collected every 1 ps in the final nanosecond of the run.

2.1.3. Calcite surface models

The calcite surface [10$\bar{1}$4] was used in this study because it is the most thermodynamically stable surface and thus the best proxy for exposed marble surfaces [40]. To confirm the validity of our computational calcite models we compared optimised bulk unit cell parameters to experimental crystallographic data (Table S6), and found that the unit cell dimensions of our DFT and MD calcite models were within 2 % of the experimental data. To create our slab model for the DFT simulations (depicted in Figure S1), we used our DFT optimised bulk structure and cut it along the {10$\bar{1}$4} plane. We used a 1 × 2 supercell with a four-layer thickness as employed in a previous study [13]. The bottom two layers of the slab were frozen in their bulk position during all geometry relaxations in order to model a semi-infinite crystal. We added a vacuum region of 25 Å to ensure no interaction occurred in the direction perpendicular to the calcite surface. For the MD simulations, we used our MD optimised bulk structure to generate an eight-layer calcite [10$\bar{1}$4] slab model with dimensions of 29.6 Å × 47.7 Å as depicted in Figure S1. The model is periodic and symmetrical, terminated by two identical surfaces. The slabs are separated by > 35 Å to prevent unwanted interactions between periodic calcite images and to ensure that the solvent could converge to bulk behaviour in the centre.

2.2. Experimental methods

2.2.1. Materials

Carrara marble was chosen as this type of marble has been widely used in sculpture and architecture since antiquity. A slab of Carrara marble was purchased from Michelangelo Imbellone s.a.s. (Italy) and wet sawn to obtain 15 × 15 × 3 mm^3 specimens. Even though the effectiveness of conservation treatments should be assessed on naturally or artificially weathered substrates to obtain a more reliable evaluation, in the present study experimental tests were performed on freshly quarried marble, with the aim to more closely resemble the system considered in the computational part, *i.e.*, calcite. In fact, alterations in marble properties induced by weathering (*e.g.*, formation of a surface gypsum crust, increases in open porosity and surface roughness) have been proven to influence the formation of calcium phosphates [41–43], hence in the present case they would have altered the mechanism under investigation (*e.g.*, the interaction between the organic additives and calcite).

Diammonium hydrogen phosphate (DAP, $(NH_4)_2HPO_4$) was kindly supplied by CTS s.r.l. (Italy). Calcium chloride dihydrate ($CaCl_2{\cdot}2H_2O$), ethanol, isopropanol, and acetone (all reagent grade) were purchased from Sigma Aldrich. All water used was deionised.

2.2.2. Treatments

Four conditions were tested, one using exclusively water as solvent and the remaining three including the additives considered in our computational study. The recipes of the four formulations are listed in Table 1. The marble specimens were treated by immersion in separate beakers containing 100 mL of solution. After immersion for a given time (24 h or 1 h, as detailed below), the specimens were rinsed with deionised water then oven-dried at 40 °C until a constant weight was reached.

Table 1
Labels and recipes of the four treatments.

Label	Recipe
Water	0.1 M DAP + 0.1 mM $CaCl_2$
Ethanol	0.1 M DAP + 0.1 mM $CaCl_2$ in 20 wt% ethanol
Isopropanol	0.1 M DAP + 0.1 mM $CaCl_2$ in 20 wt% isopropanol
Acetone	0.1 M DAP + 0.1 mM $CaCl_2$ in 20 wt% acetone

2.2.3. Characterisation

The effects of the additives on the treatment performance were evaluated in terms of:

a) *ability to favour formation of new CaP over calcite*. The surface of marble samples treated for 1 h and 24 h was observed using a field emission gun scanning electron microscope (FEG-SEM, Tescan Mira 3, working distance = 10 mm, voltage = 10 kV), after making the samples conductive by graphite evaporation. Treatment for 24 h was considered because it is the standard duration recommended in the literature, as complete HAP coatings have been found over the marble surface after such time [7]. Treatment for 1 h was tested, even though such short time is known to be insufficient to form a complete layer of CaPs over the marble surface when only water is used as a solvent, to assess whether the additives were able to accelerate CaP formation at short times, compared to the case when only water was used.
b) *ability to form a dense coating over calcite*. To obtain information on the microstructure of the coatings, cross sections were prepared by encapsulation of specimens treated for 24 h in epoxy resin and then exposure by polishing. The cross sections were observed by FEG-SEM, as described above.
c) *composition of the coatings*. The mineralogical composition of the new phases formed after treatment was determined by X-ray diffractometry (XRD), using a Malvern PANalytical Empyrean series III instrument (40 kV and 30 mA, 2θ range = 3 − 40°, step size = 0.02°, time per step = 100 sec).
d) *ability to protect marble from dissolution in simulated rain*. The protective ability of the coatings was evaluated by subjecting treated and untreated marble specimens to an accelerated acid attack test. The test consisted of immersing the specimens in 100 mL of an acidic solution of HNO_3 at pH 5, resembling the average rain pH in Europe [44–45]. The specimens were immersed in the solution for 24 h while stirring. Afterwards, the samples were rinsed with deionized water, and oven-dried at 40 °C until constant weight was reached and then observed by FEG-SEM as described above. These experimental conditions, which have been adopted in several previous studies [6,9–10,45], were selected considering that acid attack by immersion in a limited volume of solution for a few hours has been shown to provide a fairly reliable assessment of the efficacy of protective treatments, as confirmed by more sophisticated acid attack tests, involving repeated cycles of dripping of simulated rain over the specimens and drying [44].

3. Results and discussion

3.1. Computational results

The local adsorption environment at the calcite surface may influence wettability and, thus, its potential to provide sites for CaP nucleation. DFT calculations were used in this study to characterise the adsorption geometry and energy (E_{ads}) of relevant species on the calcite [10$\bar{1}$4] surface. In addition to water, three organic solvents were considered as adsorbates. Ethanol and isopropanol were chosen based on previous experimental trials showing that their use as additives

resulted in improved performance of the conservation treatment [9]. Additionally, we decided to study acetone based on its different chemistry and expected different adsorption behaviour relative to the alcohols. Furthermore, acetone is a commonly used solvent in the field of cultural heritage conservation [46].

In general, the adsorption behaviour of molecules at a solid/solution interface is heavily dependent on the properties of the solid and its exposed surface. Calcite ($CaCO_3$) is an ionic compound composed of calcium cations (Ca^{2+}) and covalently bonded carbonate anions (CO_3^{2-}), with its bulk structure consisting of Ca atoms 6-coordinate to O and O atoms 2-coordinate to Ca. Cleaving the calcite bulk to expose the [10$\bar{1}$4] surface leads to undercoordinated surface Ca and O atoms, which drive the chemical reactivity of the surface and its interaction with adsorbates. For all the molecules under study, adsorption occurs *via* the coordination between a surface Ca and $O_{adsorbate}$ (Fig. 1). Additionally, for those with a hydroxyl group, hydrogen-bonds occur between $H_{adsorbate}$ of hydroxyl group to undercoordinated surface O. Due to the multiple possible hydrogen-bonding sites on the calcite surface, several initial guesses for the adsorption geometries of adsorbates were generated by rotating the molecules around the direction perpendicular to the calcite surface in order to identify the most stable configuration. Our predicted adsorption geometries are in line with the results of a previous study performed at a similar surface coverage for water, ethanol, and acetone [14].

All E_{ads} are negative (Fig. 1), indicating that adsorption of all molecules on the calcite [10$\bar{1}$4] surface is favourable. Water and isopropanol have the same E_{ads} (-0.67 eV) and ethanol adsorbs essentially isoenergetically (-0.75 eV). This result was confirmed also for higher coverages (up to 1.0 ML) in a previous study by Okhrimenko et al. [13]. Acetone has significantly weaker adsorption (-0.30 eV) likely due to the lack of a hydroxyl group preventing the formation of stabilising hydrogen bonds with the surface, and the relatively smaller partial charge of acetone's oxygen (compared to the hydroxyl oxygen of the other adsorbates), thereby resulting in weaker bonding to surface Ca sites. Furthermore, we found that acetone adsorption is fully driven by dispersion interactions (E_{ads}-E_{disp} is + 0.02 eV). Ataman et al. studied adsorption at a similar coverage (0.13 ML) and found the same adsorption energy trend with water and ethanol adsorbing isoenergetically and more strongly than acetone [14].

Our DFT calculations shed light on the geometry of single solvent molecules adsorbing on the calcite surface and their relative adsorption strength but neglect to account for important factors that can affect the characteristics of the adsorbed layer. These include the presence of co-adsorbed species, the presence of additional solvent layers on top of the adsorbed layer, and the direct competition between water and organic solvents when both are allowed to interact with the surface at the same time. For instance, the marble surface is likely to be exposed to moisture (*i.e.*, water) prior to undergoing treatment leading to the adsorption layer being initially represented solely by water but this may change once the marble is exposed to organic solvents during treatment. In order to account for the effect of these factors and investigate this critical aspect, we undertook classical MD calculations of pure solvents (water, ethanol, isopropanol, and acetone) as well as aqueous solutions

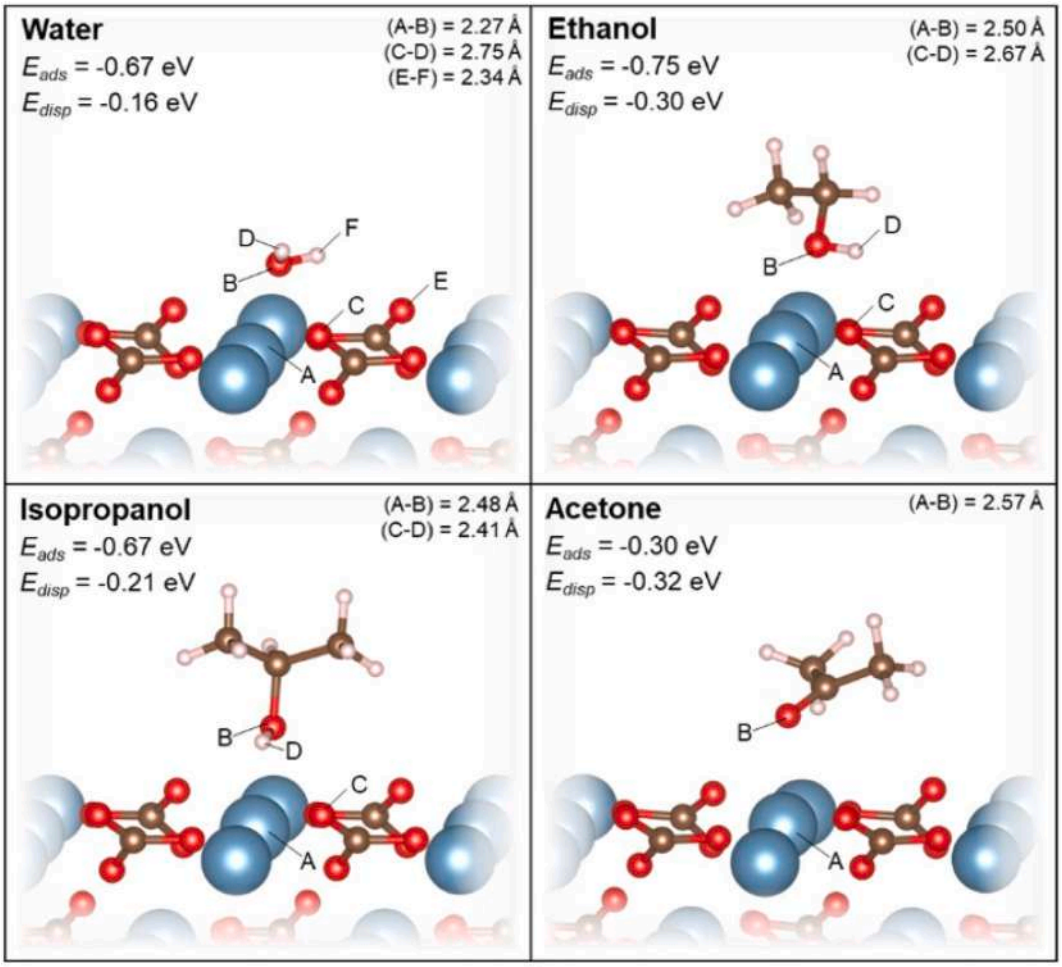

Fig. 1. Predicted adsorption energy (E_{ads}), dispersion contribution (E_{disp}) and geometry of molecules on the calcite [10$\bar{1}$4] surface at 0.25 monolayer coverage. Ca atoms are represented in cyan, O atoms in red, H atoms in off-white, and C atoms in brown. (For interpretation of the references to colour in this figure legend, the reader is referred to the web version of this article.)

of these aforementioned solvents interacting with the calcite [10$\bar{1}$4] surface. We analysed systems after 20 ns of interaction with the surface using a range of techniques: molecular trajectory snapshots and quantitative results from radial distribution functions (RDF) and density profiles.

Water exhibits two clear adsorption modes evident in Fig. 2a: in the first mode a dative bond between a surface Ca and water O is formed, and in the second a surface O forms a hydrogen-bond with a water H. The two adsorption modes are confirmed by a single peak in the RDF for both the $Ca_{calcite}$-O_{water} and $O_{calcite}$-H_{water} interactions (Fig. 3a,b). We also observe two well-defined peaks in the density profile (Fig. 4), the first at shorter distance from the surface due to the $Ca_{calcite}$-O_{water} interaction and the second at longer distance due to the $O_{calcite}$-H_{water} interaction. The location of the RDF peaks ($Ca_{calcite}$-O_{water} at 2.53 Å, $O_{calcite}$-H_{water} at 1.83 Å) and water's density profile align with the outcome of previous similar theoretical studies [13,16,26]. Compared to our DFT study, our MD study found the $Ca_{calcite}$-O_{water} interaction distance to be 0.26 Å larger, likely due to the additional interaction with co-adsorbed water molecules and those above the adsorbed layer, which are absent in our DFT model.

In contrast to water's behaviour, ethanol and isopropanol form well-ordered layers with a single adsorption mode ($Ca_{calcite}$-$O_{alcohol}$), confirmed by the single peaks in the density profiles (Fig. 4) and the intense peaks in the RDFs (Fig. 3a,b). The aliphatic tails of the adsorbed alcohols orient away from the surface forming a hydrophobic layer evident in the snapshots (Fig. 2b,c), with an extensive zero density region beyond the first peak in the density profile indicating an absence of movement from the adsorbed layer after its formation. Additionally, the snapshots and density profile of ethanol and isopropanol show evidence of structuring beyond their first adsorption layer with the non-adsorbed alcohol molecules in solution orienting their aliphatic tails towards the hydrophobic layer. This finding as well as our RDF separation distances ($Ca_{calcite}$-$O_{ethanol}$ 2.4 Å, $O_{calcite}$-$H_{ethanol}$ 1.4 Å) and density profile for ethanol are consistent with similar studies on the interaction of ethanol and the [10$\bar{1}$4] surface of calcite [16,26,47–48]. The size of the alcohols' aliphatic tails affects their ordering ability on the calcite surface, seen here with isopropanol's bulkier forked alkyl chain leading to a lower packing density (0.08 oxygen atoms/Å^3) than ethanol's straight alkyl chain (0.12 oxygen atoms/Å^3 which also represents ~ 1 ML coverage). Our finding reflects trends seen in the experimentally observed maximum coverage on the calcite [10$\bar{1}$4] surface (1 ML for ethanol, 0.75 ML for isopropanol) [13], and in an MD study by Bovet et al. which found that due to steric effects, alcohols with straight tails adsorb at 1 ML coverage and branched tails at < 1 ML [47].

Acetone exhibits two adsorption modes visually evident in the snapshot (Fig. 2d); some molecules adsorb *via* the carbonyl group ($Ca_{calcite}$-$O_{acetone}$ interaction) and the remainder *via* the alkyl group (weaker $O_{calcite}$-$H_{acetone}$ interaction). The first peak of acetone's density profile (Fig. 4, corresponding to the $Ca_{calcite}$-$O_{acetone}$ interaction) is more intense than the second peak ($O_{calcite}$-$H_{acetone}$ interaction), indicating that the $Ca_{calcite}$-$O_{acetone}$ mode is the dominant adsorption mode. There is little to no movement out of acetone's adsorption layer for molecules interacting *via* $Ca_{calcite}$-$O_{acetone}$, however, non-zero density right beyond the second peak reveals that there is movement between molecules interacting *via* $O_{calcite}$-$H_{acetone}$ and the bulk solution. This suggests that the second adsorption mode is less robust than the first, as is consistent with the weaker nature of this bond.

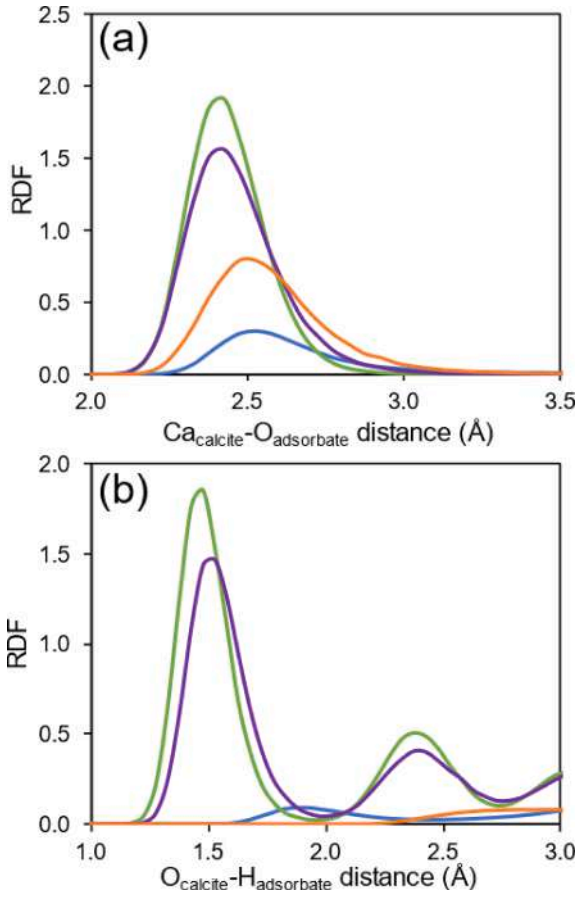

Fig. 3. (a) $Ca_{calcite}$-$O_{adsorbate}$ and (b) $O_{calcite}$-$H_{adsorbate}$ radial distribution functions for four different species adsorbing on the calcite [10$\bar{1}$4] surface: water (blue), ethanol (green), isopropanol (purple), and acetone (orange). In (b), $H_{adsorbate}$ belongs to the hydroxyl group (water, ethanol, isopropanol) or the alkyl group (acetone). (For interpretation of the references to colour in this figure legend, the reader is referred to the web version of this article.)

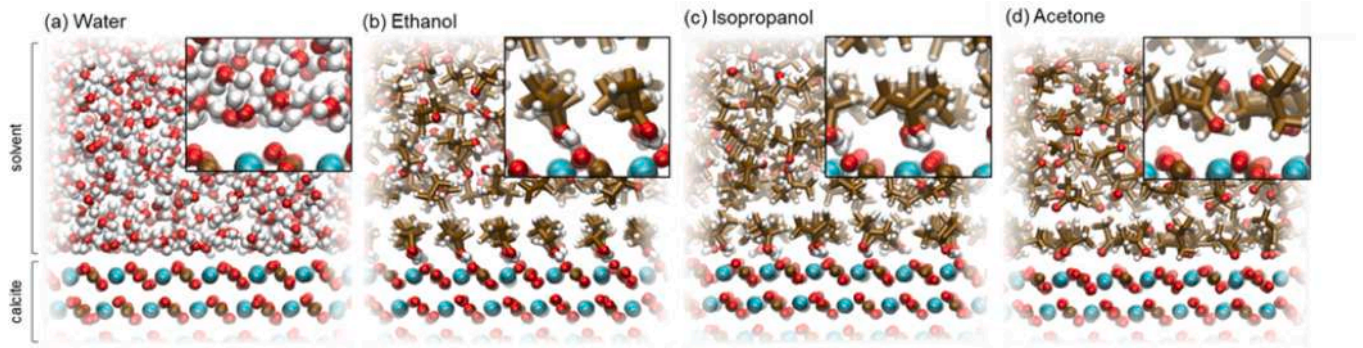

Fig. 2. Side view of pure (a) water, (b) ethanol, (c) isopropanol, and (d) acetone interacting with the [10$\bar{1}$4] calcite surface after 10 ns. Insets show the surface/solvent interaction in detail. Ca atoms are represented in cyan, O atoms in red, H atoms in off-white, and C atoms in brown. (For interpretation of the references to colour in this figure legend, the reader is referred to the web version of this article.)

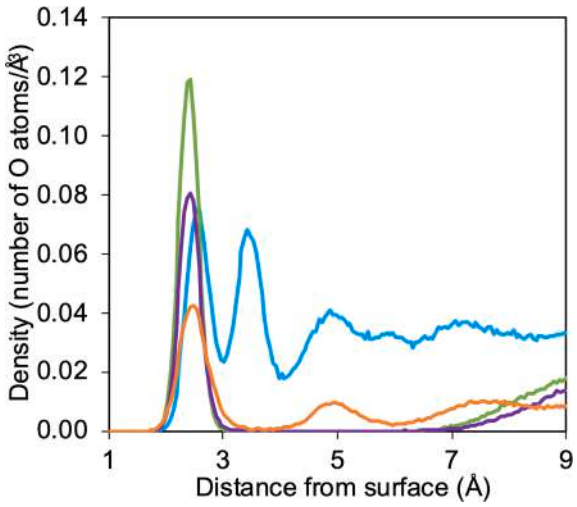

Fig. 4. Density profiles of the oxygen atoms of pure water (blue), ethanol (green), isopropanol (purple), acetone (orange) after interaction with the calcite [10$\bar{1}$4] surface along the direction perpendicular to the surface. The top-most plane of calcium atoms is defined as the surface at 0 Å. (For interpretation of the references to colour in this figure legend, the reader is referred to the web version of this article.)

Overall, we find a significant difference in the behaviour of the pure solvents interacting with the calcite surface. Water takes on bulk behaviour closer to the surface than other solvents (with a return to bulk density reached by ~ 6 Å for water, >7 Å for acetone and > 8.5 Å for the alcohols (Fig. 4)), likely due to its relatively small molecular size and ability to form an inter-connected hydrogen-bonded network. Water's dynamic adsorption environment (with molecules constantly moving between the adsorption layers and bulk solution) contrasts with the static adsorption of the alcohols, suggesting that they may be able to breach water's adsorption environment. For both water and acetone, there is less order to the $Ca_{calcite}$-$O_{solvent}$ interaction, evident in the wider first peak in the RDF (Fig. 3a) compared to the alcohols. Out of all studied solvents, acetone exhibits the sparsest coverage on calcite (0.05 oxygen atoms/Å^3), with its reduced potential packing density likely due to its tendency to orient itself in multiple adsorption configurations. The low density of acetone's adsorption layer supports the findings of our DFT study where acetone exhibited the weakest adsorption to calcite and the $Ca_{calcite}$-$O_{solvent}$ axis most parallel to the surface (Fig. 1). Evidently, a difference in functional group (carbonyl *vs.* hydroxyl) not only influences the adsorption behaviour of single molecules (as shown by our DFT results in Fig. 1), but also the properties of the solvent/solution interface and the bulk solvent, namely surface coverage, solvent mobility, and structuring in solution.

Up to this point, the predictions made by our DFT and pure solvent MD studies suggest that the alcohols and water may compete for adsorption to calcite, while acetone may not due to its weaker adsorption energy as well as its more disordered and sparser adsorption layer. The competitive adsorption behaviour across these solvents will affect the wettability of the calcite surface and hence may determine the outcome of conservation treatments for marble. To shed further light on this critical aspect, we undertook MD calculations using mixed solutions (with a constant concentration of 1:1 by number of water/organics molecules) with three controlled initial configurations: (i) water initially confined adjacent to the calcite surface with the organic solvent in the bulk solvent region, (ii) organic solvent initially confined adjacent to the calcite surface with the water in the bulk solvent region, and (iii) a random spatial arrangement. Initial configuration (i) more closely resembles the calcite surface after outdoor exposure, where the condensation of atmospheric moisture results in water adsorption on the surface.

Ethanol completely displaces water from the surface of calcite (Fig. 5a), forming a strong and well-ordered layer with a density profile similar to pure ethanol (Fig. 4). After 20 ns, all initial solvent configurations of ethanol/water result in the same adsorption profile (Fig. S2a, d). Additionally, ethanol dominates the region directly above the first adsorbed layer given the hydrophobic nature of the adsorbed layer. This finding is consistent with other MD studies of 1:1 mixtures of ethanol and water [15,26]. In a similar manner to ethanol, isopropanol displaces water almost entirely from the surface of calcite (Fig. 5b), and when isopropanol is initially adsorbed, no water is found in the adsorption layer (Fig. S2b). The zone above the adsorbed isopropanol layer is dominated by isopropanol, also similar to what was seen for the ethanol mixture (Fig. 5a). The mixed isopropanol solution exhibits a first adsorption peak and zero density region (Fig. 5b) similar to that of pure isopropanol (Fig. 4). For isopropanol/water initially configured in a random arrangement (Fig. S2e) and with water initially adsorbed (Fig. 5b), there is a small amount of water remaining at the surface (peak at ~ 2.5 Å in the density profile) which slowly reduces over the 20 ns run. This effect is due to water molecules being sterically trapped beneath bulky isopropanol tails, which are slowly released into the bulk solvent region upon the wiggling of the adsorbed isopropanol tails over the course of the simulation. In these instances, there is also a second smaller isopropanol peak at 3.5 Å in the density profile (Fig. 5b) corresponding to isopropanol molecules interacting with trapped water molecules and being slightly displaced from the surface.

In the case of the acetone/water mixtures after 20 ns, both species are present near the surface of calcite at a uniform proportion regardless of initial configuration (Fig. 5c, Fig. S2c,f). Here, water adsorbs in a similar manner to pure water (Fig. 4) with a similar profile: peaks which become less intense before returning to bulk behaviour at > 6 Å. Interestingly, when mixed with water, acetone only adsorbs *via* $O_{calcite}$-$H_{acetone}$ (confirmed by inspection of visual snapshots), which contrasts with acetone's dual adsorption modes exhibited in pure form (Fig. 4). In the mixed acetone/water adsorbed layer, water dominates by number (~0.045 atoms/Å^3 compared to ~ 0.015 atoms/Å^3 for acetone) likely due to its stronger adsorption energy (Fig. 1) and increased mobility due to small molecular size, meaning it can easily displace acetone from adsorption at the surface Ca sites ($Ca_{calcite}$-$O_{acetone}$), leading to acetone adsorbing solely *via* $O_{calcite}$-$H_{acetone}$ interactions. A lack of zero density region for both water and acetone indicates a highly dynamic adsorption environment, contrasting strongly with the behaviour of the alcohols which displaced water from the surface to form a well-ordered, highly immobile, and hydrophobic environment on the calcite [10$\bar{1}$4] surface.

Trajectory snapshots of each aqueous mixture further illustrates the differences in solvent behaviour both at the surface and in solution (Fig. 6). The alcohols exhibit the simultaneous formation of the alcohol adsorption layer and displacement of water from the surface in the first 5 ns (Fig. 6a,b), with water eventually aggregating in the bulk solvent region above the adsorbed layer resulting in low degree of mixing between water and organics. In this case, some water molecules are still visible at the surface after 5 ns, with complete displacement of water by the alcohols achieved by 20 ns for ethanol in all initial configurations (Fig. 5a), and for isopropanol with isopropanol initially adsorbed (Fig. S2b). In contrast, the acetone/water solution (Fig. 6c) shows significant amounts of both solvents in the adsorbed layer and uniform mixing in the bulk solvent region throughout the simulation (Fig. 6c). Ethanol, isopropanol, and acetone are all known to be miscible in water and our initial solvent benchmarking calculations (which excluded the presence of calcite) are consistent with this fact, showing equally good mixing for all three solvents in water; however, their different ability to compete with water for adsorption sites observed in this work results in different degrees of mixing in the local environment near the surface/solution interface. Overall, these differences across the three organic solvents may affect the wettability of the calcite surface which in turn could affect CaP nucleation at the surface and the treatment outcome.

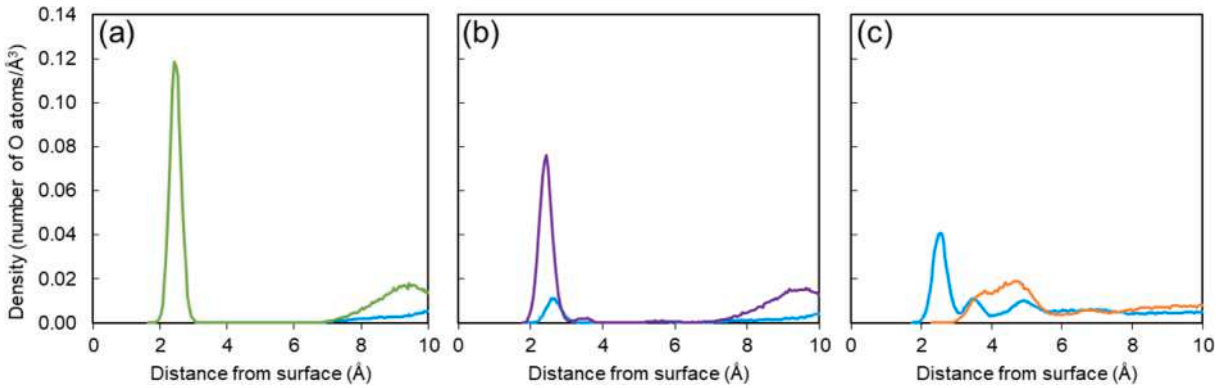

Fig. 5. Density profiles of the oxygen atoms of 1:1 solutions of water (blue) and (a) ethanol (green), (b) isopropanol (purple) and (c) acetone (orange) after interaction with the calcite [10$\bar{1}$4] surface along the direction perpendicular to the surface. The top-most plane of calcium atoms is defined as the surface at 0 Å. All simulations were initialised with water confined adjacent to the calcite surface and the organic solvent in the bulk solvent region. (For interpretation of the references to colour in this figure legend, the reader is referred to the web version of this article.)

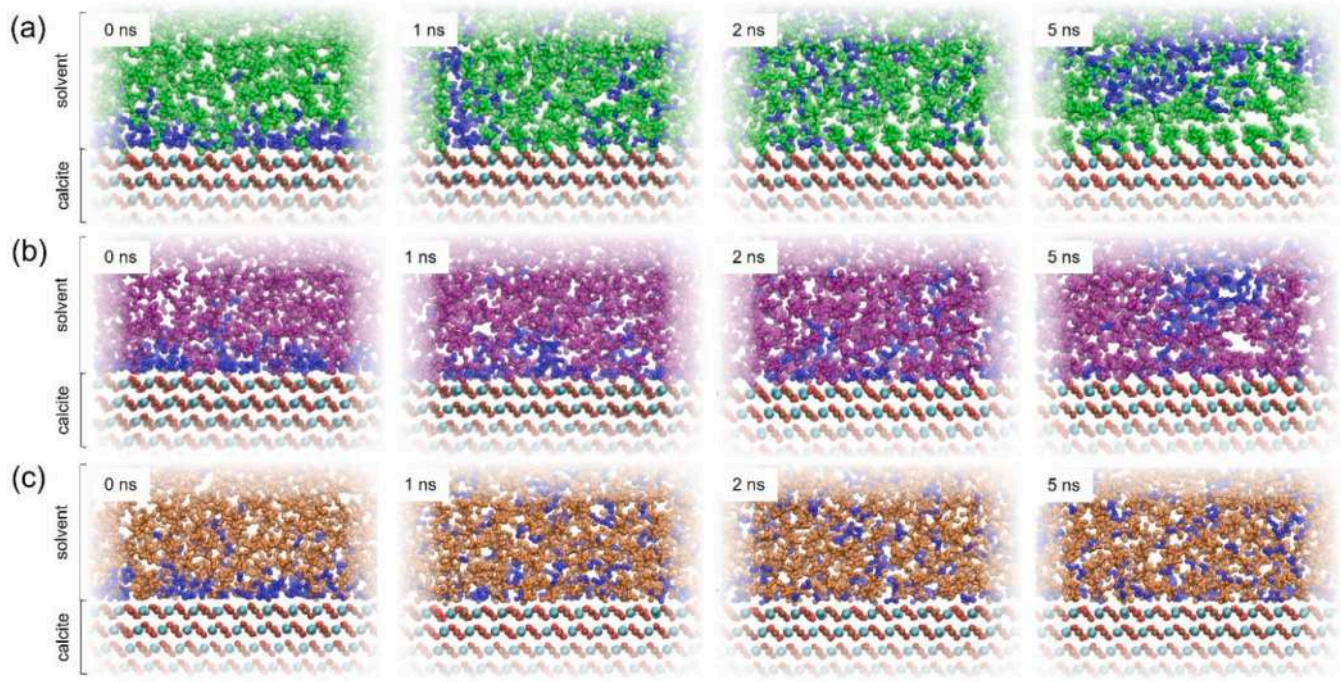

Fig. 6. Side view of the [10$\bar{1}$4] calcite surface captured after interaction with 1:1 mixtures of water and (a) ethanol, (b) isopropanol and (c) acetone. The initial solvent configurations were with water initially confined adjacent to the calcite surface and the organic solvent in the bulk solvent region. Calcite Ca atoms are represented in cyan, calcite O atoms in red, calcite C atoms in brown, water molecules in blue, ethanol molecules in green, isopropanol molecules in purple, and acetone molecules in orange. Snapshot times are measured from the beginning of the production run. (For interpretation of the references to colour in this figure legend, the reader is referred to the web version of this article.)

This aspect is examined experimentally in the next section.

3.2. Experimental results

The ability of the organic additives to promote formation of new CaP was first assessed by observing treated surfaces by SEM. Compared to water, all three organic additives favour formation of new CaP over the marble surface, as shown in Fig. 7. After 1 h, isolated CaP clusters are visible in the case of water, while a more continuous CaP coating is present with the three additives, which all appear to speed up the CaP formation, without a clear difference among them. After 24 h, a continuous (but cracked) layer is formed in all conditions, including water. Cracking is thought to occur during drying, as consequence of stress arising in the coatings, which are hence suspected to contain pores [49–50].

To characterise the microstructure of the coatings, cross sections were observed by SEM and the presence of phosphorus (linked to formation of new CaP phases) was traced by EDS. As illustrated in Fig. 8, after 24 h a surface coating with a few micrometres thickness is formed in all conditions. The coating is less uniform and continuous when only water is present, compared to when the additives are used. The coating appears thicker in the case of isopropanol and acetone but overall no dramatic differences among the additives are observed. In terms of porosity of the coatings, no clear difference could be detected among the various samples. For a conclusive evaluation of the coating porosity, analyses by focused ion beam (FIB) microscopy would be needed. Such work is currently in progress.

Based on results of X-ray diffraction performed on the sample surface

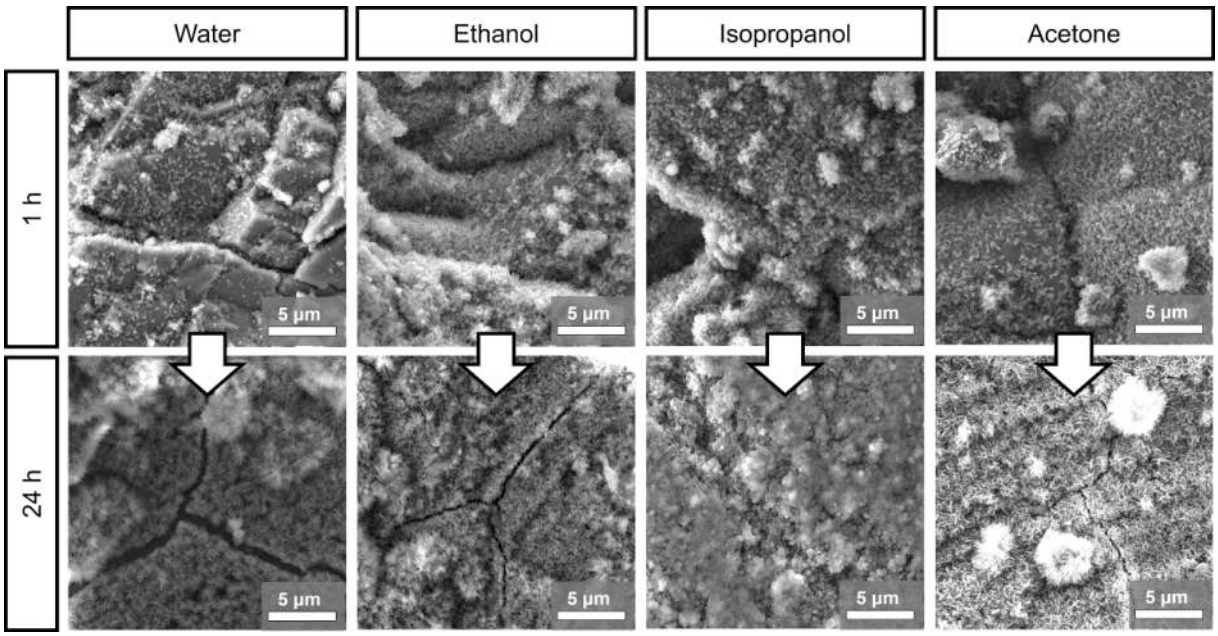

Fig. 7. SEM images of the surface of marble specimens treated with the solutions of diammonium hydrogen phosphate containing the various additives for the indicated times.

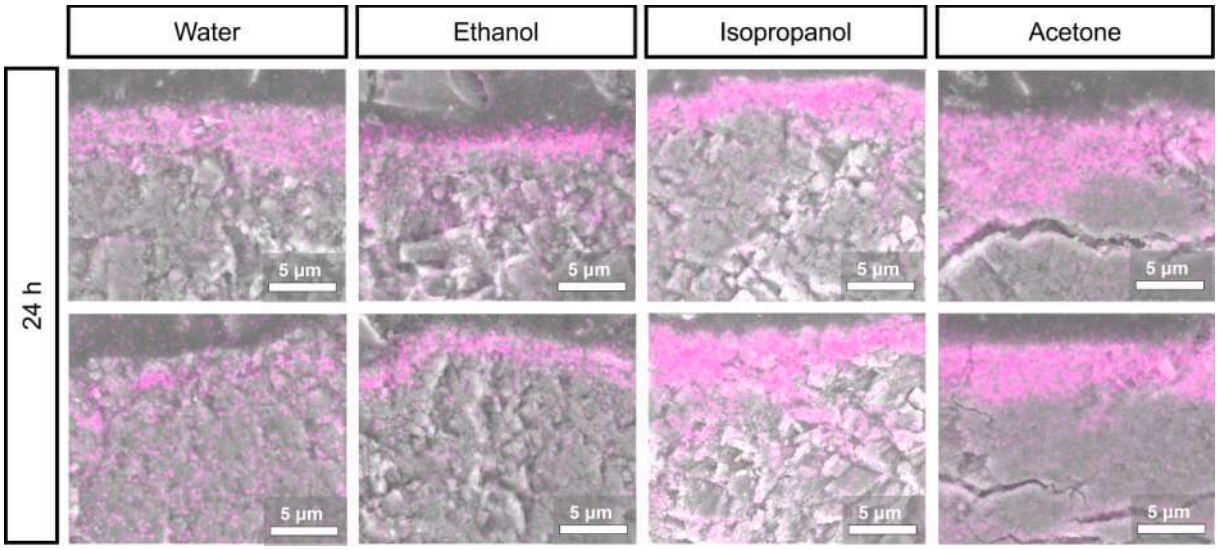

Fig. 8. SEM images of cross sections of marble specimens treated with the solutions of diammonium hydrogen phosphate containing the various additives for 24 h (the pink colour indicates the presence of phosphorous from signal by EDS). (For interpretation of the references to colour in this figure legend, the reader is referred to the web version of this article.)

(Fig. 9), calcite ($CaCO_3$, ICDD 01-083-1762) is the only phase present in the untreated reference. All the treatments, independently of the solvent used, led to formation of apatite phases, most likely carbonated hydroxyapatite ($Ca_{10}(PO_4)_3(CO_3)_3(OH)_2$, ICDD 00-019-0272), although formation of stoichiometric hydroxyapatite ($Ca_{10}(PO_4)_6(OH)_2$, ICDD 96-900-2214) cannot be excluded. Formation of carbonate hydroxyapatite, which is consistent with previous findings of treatment of calcitic substrates with aqueous DAP solutions [51–52], is a consequence of the presence of carbonate ions originated from the calcitic substrate and from atmospheric CO_2, which are incorporated into the hydroxyapatite lattice. Formation of other CaP phases, such as octacalcium phosphate (OCP, $Ca_8H_2(PO_4)_6{\cdot}5H_2O$) or brushite ($CaHPO_4{\cdot}2H_2O$), can be excluded, as both these minerals have characteristic peaks that are easily distinguishable from those of hydroxyapatite.

Considering that the protective ability of a coating depends on its composition, continuity over the marble surface, and microstructure, the protective ability was assessed as a further indirect indication of the effects of the organic additives. As shown in Fig. 10, SEM observation of the sample surface after the acid attack test showed that, as expected, untreated marble is severely etched during the test. When only water is used as solvent, the resulting protective layer is damaged during the acid attack test, as revealed by the presence of extended bare areas after the test. When using the three organic additives, sensibly lower damage to the coating is found at the end of the test (as evidenced by phosphorus maps), without dramatic differences among the various solvents.

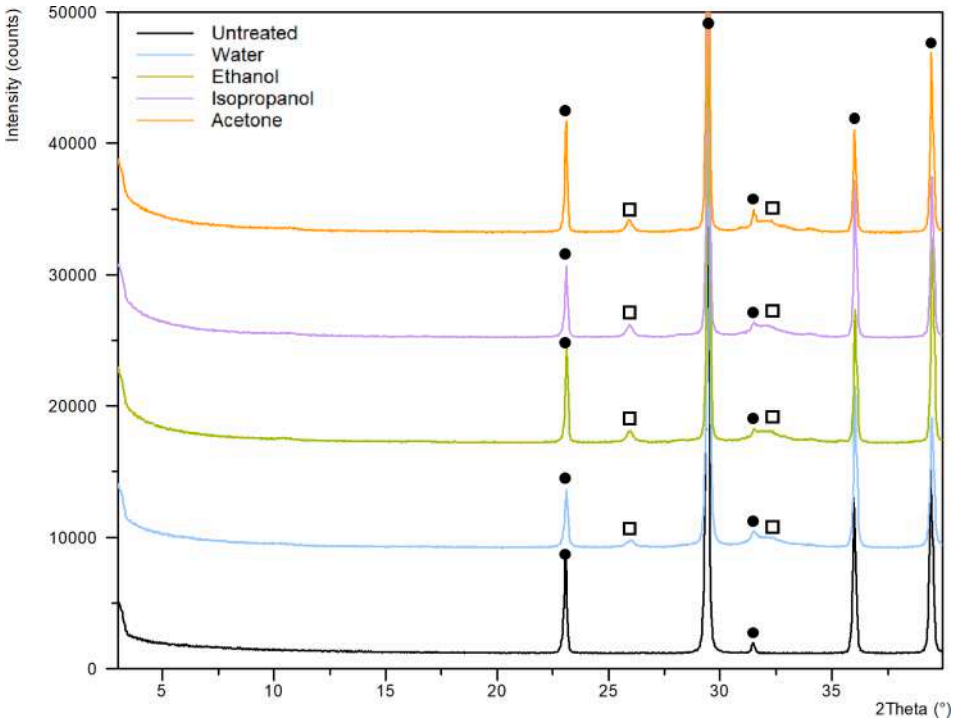

Fig. 9. Mineralogical composition of the coatings: • = calcite, □ = apatite phases.

3.3. Discussion

Our computational findings indicate that alcohols and acetone have a different interaction with the calcite surface and a different ability to displace water. Nonetheless, our experimental findings show that all organic additives improved the treatment outcome compared to water alone, without a dramatic difference between them. As a result, we conclude that the adsorption of the additive on the surface does not play a major role in determining the outcome of the conservation treatment. On the contrary, other factors must be playing a role. These factors may include the ability of the additive to weaken the hydration sphere of the phosphate ions in solution [11] as well as the adsorption of the additives on the new CaP growth. There is currently a lack of data in the literature concerning these aspects and computational work is currently in progress in our group to elucidate them.

The similar treatment outcome yet different adsorption behaviour of the additives might also be explained by the fact that CaP crystallisation is not only occurring on the planar $[10\bar{1}4]$ surface of calcite, but also on vicinal (stepped) surfaces which may occur naturally. In fact, Keller et al. studied the adsorption of ethanol and water mixtures on the planar $[10\bar{1}4]$ surface and stepped surfaces of calcite and found that, when the density of stepped faces increased, ethanol adsorption became less dominant and the adsorption of water to these stepped surfaces improved [15]. Due to natural surface imperfections of calcite, the alcoholic hydrophobic layer may not be as robust as predicted for the planar $[10\bar{1}4]$ surface, thus explaining why water adsorption and CaP formation can occur equally well independently from the organic additive used. An alternative explanation for this observation, is that the surface of the calcite is not composed solely of carbonate and calcium ions. In fact, it has been suggested that at neutral pH the surface will be partially terminated by hydrogen carbonate, which would lead to less calcium adsorption sites being present [53]. Under these conditions, the adsorption behaviour of water and the organic solvents may change, potentially leading to water dominating the adsorption layer. These aspects will be the subject of future investigations in our group.

4. Conclusions

The present study was aimed at elucidating the effect that organic additives (ethanol, isopropanol, and acetone) have on the formation of CaP for marble conservation using a range of computational and experimental techniques. Overall, our computational results show that acetone has weaker adsorption than the alcohols and lacks the ability to displace water from the calcite surface, suggesting that acetone will not make the surface hydrophobic, thus potentially aiding ion transport to the surface resulting in an improved CaP protective layer. This is in contrast to the alcohols which form a well-ordered and hydrophobic adsorbed layer at the surface. On the other hand, our experimental results indicate that all organic additives have a positive effect on CaP coating formation, with no major difference observed experimentally between the use of acetone or the alcohols when considering the composition, density, and protective efficacy of the final coating, at least in the adopted experimental conditions. Combined, the computational and experimental results suggest that the different behaviour of the additives at the calcite surface does not, in fact, have a major effect on conservation treatment outcomes. Instead, treatment improvement when using organic additives may be due to other factors such as the ability of an additive to weaken the hydration sphere of phosphates in solution, an aspect that is currently under investigation in our group.

CRediT authorship contribution statement

Antonia E. Papasergio: Investigation, Software, Formal analysis, Validation, Visualization, Writing – original draft, Writing – review & editing. **Greta Ugolotti:** Investigation, Formal analysis, Visualization, Writing – review & editing. **Enrico Sassoni:** Conceptualization, Methodology, Resources, Investigation, Supervision, Formal analysis, Visualization, Writing – original draft, Writing – review & editing. **Martina Lessio:** Conceptualization, Methodology, Resources, Supervision, Formal analysis, Supervision, Writing – original draft, Writing – review & editing.

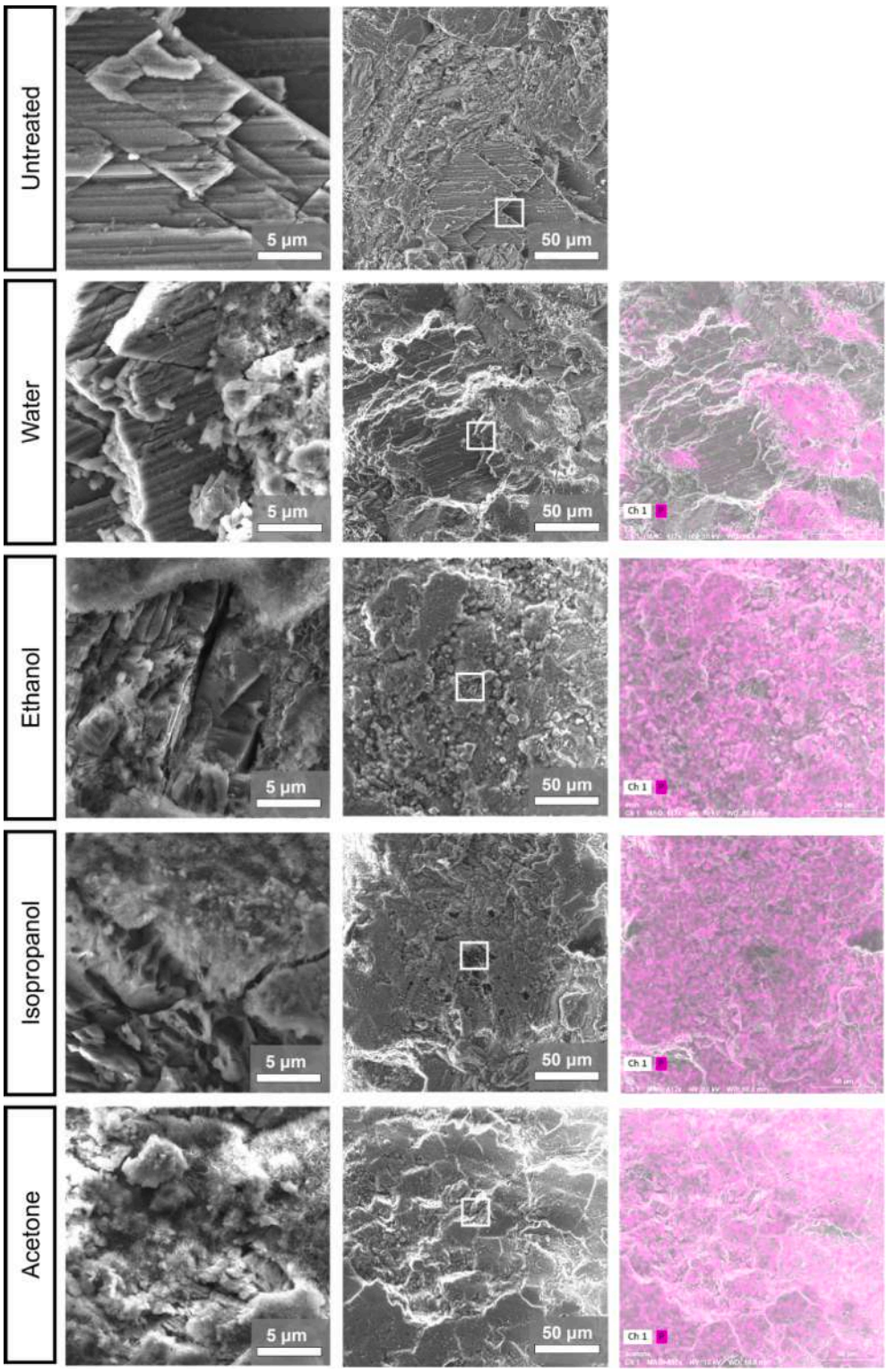

Fig. 10. SEM images of the surface of marble specimens untreated and treated with solutions of diammonium hydrogen phosphate containing the various additives, after the acid attack test. The white squares in the second column of images indicate the areas where the magnification displayed in the first column was acquired. The EDS maps (last column) show the presence of phosphorus in the areas shown in the second column.

Declaration of Competing Interest

The authors declare that they have no known competing financial interests or personal relationships that could have appeared to influence the work reported in this paper.

Data availability

Data will be made available on request.

Acknowledgements

The authors acknowledge use of computational resources and services from the National Computational Infrastructure (NCI), and the computational cluster Katana supported by Research Technology Services at UNSW Sydney. We would like to thank Dr P. V. G. M. Rathnayake for help with the computational aspects of this study. Centro Ceramico (Bologna) is gratefully acknowledged for access to XRD.

Appendix A. Supplementary material

Supplementary data to this article can be found online at https://doi.org/10.1016/j.apsusc.2023.156438.

References

[1] L. Brečević, D. Kralj, On Calcium Carbonates: From Fundamental Research to Application, Croatica Chem. Acta (2007) 467–484.
[2] N.K. Dhami, M.S. Reddy, M.S. Mukherjee, Biomineralization of Calcium Carbonates and Their Engineered Applications: A Review, Front. Microbiol. (2013), https://doi.org/10.3389/fmicb.2013.00314.
[3] M. Chaussemier, E. Pourmohtasham, D. Gelus, N. Pécoul, H. Perrot, J. Lédion, H. Cheap-Charpentier, O. Horner, State of Art of Natural Inhibitors of Calcium Carbonate Scaling. A Review Article, *Desalination* 356 (2015) 47–55, https://doi.org/10.1016/J.DESAL.2014.10.014.
[4] D.G. Kanellopoulou, P.G. Koutsoukos, The Calcitic Marble/Water Interface: Kinetics of Dissolution and Inhibition with Potential Implications in Stone Conservation, Langmuir 19 (14) (2003) 5691–5699, https://doi.org/10.1021/la034015x.
[5] P.V. Brady, (Ed. *Physics and Chemistry of Mineral Surfaces*, 1st ed.; Brady, P. V., Ed.; CRC Press: Boca Raton, 1996. 10.1201/9781003068945.
[6] S. Naidu, J. Blair, G.W. Scherer, Acid-Resistant Coatings on Marble, J. Am. Ceram. Soc. 99 (10) (2016) 3421–3428, https://doi.org/10.1111/jace.14355.
[7] E. Sassoni, Hydroxyapatite And Other Calcium Phosphates for the Conservation of Cultural Heritage: A Review, Materials (Basel) 11 (4) (2018), https://doi.org/10.3390/ma11040557.
[8] E. Sassoni, S. Naidu, G.W. Scherer, The Use of Hydroxyapatite as a New Inorganic Consolidant for Damaged Carbonate Stones, J. Cult. Herit. 12 (4) (2011) 346–355, https://doi.org/10.1016/j.culher.2011.02.005.
[9] E. Sassoni, G. Graziani, E. Franzoni, G.W. Scherer, Calcium Phosphate Coatings for Marble Conservation: Influence of Ethanol and Isopropanol Addition to the Precipitation Medium on the Coating Microstructure and Performance, Corros. Sci. 2018 (136) (October 2017) 255–267, https://doi.org/10.1016/j.corsci.2018.03.019.
[10] G. Graziani, E. Sassoni, E. Franzoni, G.W. Scherer, Hydroxyapatite Coatings for Marble Protection: Optimization of Calcite Covering and Acid Resistance, Appl. Surf. Sci. 368 (2016) 241–257, https://doi.org/10.1016/j.apsusc.2016.01.202.
[11] M.S. Tung, T.J. O'Farrell, Effect of Ethanol on the Formation of Calcium Phosphates, Colloids Surfaces A Physicochem. Eng. Asp. 110 (2) (1996) 191–198, https://doi.org/10.1016/0927-7757(95)03450-1.
[12] E. Lerner, R. Azoury, S. Sarig, Rapid Precipitation of Apatite from Ethanol-Water Solution, J. Cryst. Growth 97 (3–4) (1989) 725–730, https://doi.org/10.1016/0022-0248(89)90576-9.
[13] D.V. Okhrimenko, J. Nissenbaum, M.P. Andersson, M.H.M. Olsson, S.L.S. Stipp, Energies of the Adsorption of Functional Groups to Calcium Carbonate Polymorphs: The Importance of -OH and -COOH Groups, Langmuir 29 (35) (2013) 11062–11073, https://doi.org/10.1021/la402305x.
[14] E. Ataman, M.P. Andersson, M. Ceccato, N. Bovet, S.L.S. Stipp, Functional Group Adsorption on Calcite: I. Oxygen Containing and Nonpolar Organic Molecules, J. Phys. Chem. C 120 (30) (2016) 16586–16596, https://doi.org/10.1021/acs.jpcc.6b01349.
[15] K.S. Keller, M.H.M. Olsson, M. Yang, S.L.S. Stipp, Adsorption of Ethanol and Water on Calcite: Dependence on Surface Geometry and Effect on Surface Behavior, Langmuir 31 (13) (2015) 3847–3853, https://doi.org/10.1021/LA504319Z.
[16] K.K. Sand, M. Yang, E. Makovicky, D.J. Cooke, T. Hassenkam, K. Bechgaard, S.L.S. Stipp, Binding of Ethanol on Calcite: The Role of the OH Bond and Its Relevance to Biomineralization. *Langmuir* **2010**, *26* (19), 15239–15247. 10.101/la101136j.
[17] G. Kresse, J. Furthmüller, Efficiency of Ab-Initio Total Energy Calculations for Metals and Semiconductors Using a Plane-Wave Basis Set, Comput. Mater. Sci. 6 (1996) 15–50, https://doi.org/10.1016/0927-0256(96)00008-0.
[18] G. Kresse, J. Furthmüller, Efficient Iterative Schemes for Ab Initio Total-Energy Calculations Using a Plane-Wave Basis Set, Phys. Rev. B 54 (1996) 11169–11186, https://doi.org/10.1103/PhysRevB.54.11169.
[19] G. Kresse, J. Hafner, Ab Initio Molecular Dynamics for Open-Shell Transition Metals, Phys. Rev. B 48 (1993) 13115–13118, https://doi.org/10.1103/PhysRevB.48.13115.
[20] P. Hohenberg, W. Kohn, Inhomogeneous Electron Gas, Phys. Rev. 136 (1964) B864, https://doi.org/10.1103/PhysRev.136.B864.
[21] W. Kohn, L.J. Sham, Self-Consistent Equations Including Exchange and Correlation Effects, Phys. Rev. 140 (1965) A1133, https://doi.org/10.1103/PhysRev.140.A1133.
[22] J. Perdew, K. Burke, M. Ernzerhof, Generalized Gradient Approximation Made Simple, Phys. Rev. Lett. 77 (1996) 3865, https://doi.org/10.1103/PhysRevLett.77.3865.
[23] G. Kresse, D. Joubert, From Ultrasoft Pseudopotentials to the Projector Augmented Wave Method, Phys. Rev. B 59 (1999) 1758, https://doi.org/10.1103/PhysRevB.59.1758.
[24] S. Grimme, S. Ehrlich, L. Goerigk, Effect of the Damping Function in Dispersion Corrected Density Functional Theory, J. Comput. Chem. 32 (2011) 1456–1465, https://doi.org/10.1002/jcc.21759.
[25] H.J. Monkhorst, J.D. Pack, Special Points for Brillouin-Zone Integrations, Phys. Rev. B 13 (1976) 5188.
[26] D.J. Cooke, R.J. Gray, K.K. Sand, S.L.S. Stipp, J.A. Elliott, Interaction of Ethanol and Water with the 1014 Surface of Calcite, Langmuir 26 (18) (2010) 14520–14529, https://doi.org/10.1021/la100670k.
[27] A. Pavese, M. Catti, G.D. Price, R.A. Jackson, Interatomic Potentials for CaCO3 Polymorphs (Calcite and Aragonite), Fitted to Elastic and Vibrational Data, Phys Chem Miner. 19 (1992) 80–87.
[28] A. Pavese, M. Catti, S.C. Parker, A. Wall, Modelling of the Thermal Dependence of Structural and Elastic Properties of Calcite, CaCO 3, Phys Chem Miner. 23 (1996) 89–93.
[29] J. Wang, R.M. Wolf, J.W. Caldwell, P.A. Kollman, D.A. Case, Development and Testing of a General Amber Force Field, J. Comput. Chem. 25 (9) (2004) 1157–1174, https://doi.org/10.1002/jcc.20035.
[30] F. Neese, The ORCA Program System, Wiley Interdiscip. Rev. Comput. Mol. Sci. (2012), https://doi.org/10.1002/wcms.81.
[31] F. Neese, Software Update: The ORCA Program System, Version 4.0. *Wiley Interdiscip*, Rev. Comput. Mol. Sci. (2018), https://doi.org/10.1002/wcms.1327.
[32] D.J. Price, C.L. Brooks, A Modified TIP3P Water Potential for Simulation with Ewald Summation, J. Chem. Phys. 121 (20) (2004) 10096–10103, https://doi.org/10.1063/1.1808117.
[33] P.P. Ewald, Die Berechnung Optischer Und Elektrostatischer Gitterpotentiale, Annalen der Physik 369 (3) (1921) 253–287, https://doi.org/10.1002/ANDP.19213690304.
[34] C.L. Freeman, J.H. Harding, D.J. Cooke, J.A. Elliott, J.S. Lardge, D.M. Duffy, New Forcefields for Modeling Biomineralization Processes, J. Phys. Chem. C 111 (32) (2007) 11943–11951, https://doi.org/10.1021/jp071887p.
[35] S. Kim, M.C. Marcano, U. Becker, Mechanistic Study of Wettability Changes on Calcite by Molecules Containing a Polar Hydroxyl Functional Group and Nonpolar Benzene Rings, Langmuir 35 (7) (2019) 2527–2537, https://doi.org/10.1021/ACS.LANGMUIR.8B03666.
[36] L. Martinez, R. Andrade, E.G. Birgin, J.M. Martínez, PACKMOL: A Package for Building Initial Configurations for Molecular Dynamics Simulations, J. Comput. Chem. 30 (13) (2009) 2157–2164, https://doi.org/10.1002/JCC.21224.
[37] J.M. Martínez, L. Martínez, Packing Optimization for Automated Generation of Complex System's Initial Configurations for Molecular Dynamics and Docking, J. Comput. Chem. 24 (7) (2003) 819–825, https://doi.org/10.1002/JCC.10216.
[38] A.P. Thompson, H.M. Aktulga, R. Berger, D.S. Bolintineanu, W.M. Brown, P.S. Crozier, P.J. in 't Veld, A. Kohlmeyer, S.G. Moore, T.D. Nguyen, R. Shan, M.J. Stevens, J. Tranchida, C. Trott, S.J. Plimpton, LAMMPS - a Flexible Simulation Tool for Particle-Based Materials Modeling at the Atomic, Meso, and Continuum Scales. Comput. Phys. Commun. 271 (2022) 108171. 10.1016/J.CPC.2021.108171.
[39] W. Humphrey, A. Dalke, K. Schulten, VMD: Visual Molecular Dynamics, J. Mol. Graph. 14 (1) (1996) 33–38, https://doi.org/10.1016/0263-7855(96)00018-5.
[40] W. Sekkal, A. Zaoui, Nanoscale Analysis of the Morphology and Surface Stability of Calcium Carbonate Polymorphs, Sci. Rep. 3 (2013), https://doi.org/10.1038/srep01587.
[41] E. Sassoni, G. Graziani, E. Franzoni, Repair of Sugaring Marble by Ammonium Phosphate: Comparison with Ethyl Silicate and Ammonium Oxalate and Pilot Application to Historic Artifact, Mater. Des. 88 (2015) 1145–1157, https://doi.org/10.1016/j.matdes.2015.09.101.
[42] E. Sassoni, G. Graziani, E. Franzoni, G.W. Scherer, Conversion of Calcium Sulfate Dihydrate into Calcium Phosphates as a Route for Conservation of Gypsum Stuccoes and Sulfated Marble, Constr. Build. Mater. 170 (2018) 290–301, https://doi.org/10.1016/j.conbuildmat.2018.03.075.
[43] E. Sassoni, G. Graziani, E. Franzoni, G.W. Scherer, New Method for Controllable Accelerated Aging of Marble: Use for Testing of Consolidants, J. Am. Ceram. Soc. 101 (9) (2018) 4146–4157, https://doi.org/10.1111/jace.15522.
[44] G. Graziani, E. Sassoni, G.W. Scherer, E. Franzoni, Resistance to Simulated Rain of Hydroxyapatite- and Calcium Oxalate-Based Coatings for Protection of Marble against Corrosion, Corros. Sci. 127 (2017) 168–174, https://doi.org/10.1016/j.corsci.2017.08.020.
[45] E. Sassoni, G. Masi, M.C. Bignozzi, E. Franzoni, Electrodeposition of Hydroxyapatite Coatings for Marble Protection: Preliminary Results, Coatings 9 (3) (2019) 207, https://doi.org/10.3390/coatings9030207.
[46] A. Vinçotte, E. Beauvoit, N. Boyard, E. Guilminot, Effect of Solvent on PARALOID® B72 and B44 Acrylic Resins Used as Adhesives in Conservation, Herit. Sci. 7 (1) (2019) 1–9, https://doi.org/10.1186/s40494-019-0283-9.
[47] N. Bovet, M. Yang, M.S. Javadi, S.L.S. Stipp, Interaction of Alcohols with the Calcite Surface. Phys. Chem. Chem. Phys. 17 (5) (2015) 3490–3496. 10.1039/C4CP05235H.
[48] H. Söngen, S.J. Schlegel, Y. Morais Jaques, J. Tracey, S. Hosseinpour, D. Hwang, R. Bechstein, M. Bonn, A.S. Foster, A. Kühnle, E.H.G. Backus, Water Orientation at the Calcite-Water Interface, J. Phys. Chem. Lett. 12 (31) (2021) 7605–7611, https://doi.org/10.1021/acs.jpclett.1c01729.

[49] S. Naidu, G.W. Scherer, Nucleation, Growth and Evolution of Calcium Phosphate Films on Calcite, J. Colloid Interface Sci. 435 (2014) 128–137, https://doi.org/10.1016/j.jcis.2014.08.018.
[50] A.G. Evans, M.D. Drory, M.S. Hu, The Cracking and Decohesion of Thin Films, *J. Mater. Res.*. Springer January 31 (1988) 1043–1049, https://doi.org/10.1557/JMR.1988.1043.
[51] E. Possenti, C. Colombo, C. Conti, L. Gigli, M. Merlini, J.R. Plaisier, M. Realini, D. Sali, G.D. Gatta, Diammonium Hydrogenphosphate for the Consolidation of Building Materials. Investigation of Newly-Formed Calcium Phosphates, Constr. Build. Mater. 195 (2019) 557–563, https://doi.org/10.1016/J.CONBUILDMAT.2018.11.077.
[52] E. Possenti, C. Colombo, D. Bersani, M. Bertasa, A. Botteon, C. Conti, P.P. Lottici, M. Realini, New Insight on the Interaction of Diammonium Hydrogenphosphate Conservation Treatment with Carbonatic Substrates: A Multi-Analytical Approach, Microchem. J. 127 (2016) 79–86, https://doi.org/10.1016/J.MICROC.2016.02.008.
[53] H. Heinz, H. Ramezani-Dakhel, Simulations of Inorganic-Bioorganic Interfaces to Discover New Materials: Insights, Comparisons to Experiment, Challenges, and Opportunities, Chem. Soc. Rev. 45 (2) (2016) 412–448, https://doi.org/10.1039/c5cs00890e.